

A new 5C pyrrhotite¹

RUTH F. ENGEL, DONALD R. PEACOR AND WILLIAM C. KELLY

Department of Geology and Mineralogy, The University of Michigan
Ann Arbor, Michigan, 48109

Abstract

A unique pyrrhotite, having a new 5C type superstructure, has been found in a specimen from an alpine hydrothermal vein. Precession photographs show that it differs from the previously-described 5C pyrrhotites in that the superstructure reflections are offset from Bragg positions. The composition is Fe_9S_{10} , and this phase is thus a polymorph of so-called hexagonal pyrrhotite of that composition. Fluid inclusion work indicates that it formed at a temperature of at least 160–170°C and that it is highly unlikely that it was quenched from that temperature.

Introduction

In the course of a routine survey of natural pyrrhotites, the authors chanced upon a remarkable specimen, from an alpine vein at Uri, Switzerland, in which small pyrrhotite crystals gave a unique diffraction pattern with superstructure reflections defining a new 5C type. Systematic studies were undertaken to define the new pyrrhotite and to specify the natural conditions under which it had formed and survived.

All 5C pyrrhotites described so far in the literature have their superlattice reflections in Bragg positions (Carpenter and Desborough, 1964; Corlett, 1968; Morimoto *et al.*, 1971; Morimoto *et al.*, 1975a). These 5C pyrrhotites are considered to be a special case of the NC type with an integral value of N and stoichiometric composition. Furthermore, such pyrrhotite is a stable phase at low temperature and so occurs abundantly in many localities (Morimoto *et al.*, 1975a). Data obtained from our pyrrhotite indicate that at least the 5C type structure can be found in nature with other than the previously-reported superstructure.

Diffraction data and chemical analysis

Careful crystallographic work was undertaken in order to obtain a complete characterization of this new pyrrhotite. Single-crystal work was carried out using standard precession techniques, and a represen-

tative photograph is reproduced in Figure 1a. After long exposure with $\text{CuK}\alpha$ radiation no reflections of kinds other than represented on the photograph could be observed. The superstructure reflections define a supercell of dimensions $\sim 2A$ 5C. They are very slightly equally displaced about a line parallel to c^* at $1/2A^*$. The interval Δh (Fig. 1b) is used to define the value of N of the NA 3C type ($N = 2a^*/\Delta h$). Nakazawa and Morimoto (1971) determined that N varies continuously from 90 to 40 with decreasing temperature. Kissin (1974) found a value of N as high as 105 for a crystal synthesized out of the NA 3C field of stability and formed by quenching the starting material from 700°C. In general he observed little systematic variation of the N value. For this study we adopted the definition of N as given above, even though our material is a 5C pyrrhotite and this nomenclature is currently used for NA 3C pyrrhotites. In this case the value of N is 37. We note that our pyrrhotite could be referred to as NA 5C pyrrhotite, but we avoid that nomenclature in order that there be no confusion with NA 3C pyrrhotites.

In order to see if the composition commonly associated with the 5C type structure, as established by Morimoto *et al.* (1975a), also holds for this new pyrrhotite, quantitative chemical analyses were obtained. The compositions of two crystals (Table 1) were determined by electron microprobe analysis, with synthetic troilite (FeS), Ni spinel (NiAl_2O_4), Co spinel (CoAl_2O_4), and metallic Cu as standards. The pyrrhotites were analyzed for Fe, S, Co, Ni, and Cu at 15 kV and $0.009\mu\text{a}$ sample current. The data for

¹ Contribution No. 342 from the Mineralogical Laboratory, Department of Geology and Mineralogy, The University of Michigan.

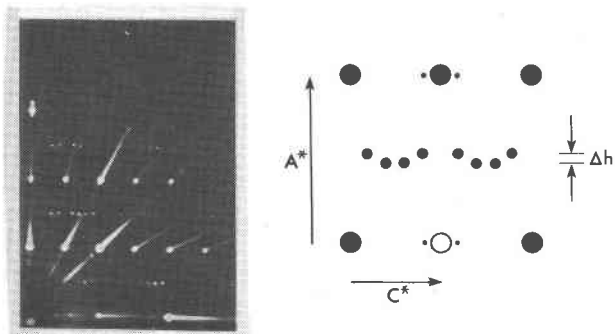


Fig. 1. (a) One quadrant of the zero-level single-crystal precession photograph of the $h0l^*$ plane of the unique 5C pyrrhotite. The dark spot at the lower left-hand corner is the beam stop. MoK α radiation. (b) Diagram of the $h0l^*$ plane of Fig. 1a.

the two analyses were reduced by a version of the program EMPADR (Rucklidge and Gasparrini, 1969) giving S:(Fe+Ni+Co) ratios of 1.120 and S:(Fe+Ni+Co+Cu) of 1.105, respectively. The 5C type has the composition Fe₉S₁₀, corresponding to the ratio of S:Fe of 1.1111. This compares very well with our results, the average of which is 1.112.

Cell parameters were determined from powder diffractometer scans obtained with monochromatized CuK α radiation and quartz as an internal standard. Least-squares refinements of the dimensions were carried out with the program LCLSQ (Burnham, 1965). The subcell lattice parameters so obtained are $A = 3.442(5)$ and $C = 5.731(3)A$. The experimentally-obtained values for the composition and cell dimensions coincide, within one standard error, with the values for a 5C pyrrhotite as determined using the t -N, V -N and t - x (t = cell translation, V = cell volume, N = C axis repeat, and x = atomic percent of iron) curves for NC pyrrhotites (Morimoto *et al.*, 1975a), thus verifying that the composition is Fe₉S₁₀.

In order to see if more crystals of this highly unusual pyrrhotite could be found, we obtained a sample with pyrrhotite from the same locality, which we will refer to as specimen 2. Several crystals, representing two ages of formation, as discussed further on, were X-rayed and gave superstructure reflections of the 5.5C (also referred to as 11C) and 4C types. These structures will not be further discussed as they are fully described in the literature (Morimoto *et al.*, 1971; Morimoto *et al.*, 1975b; Tokonami *et al.*, 1972; Nakazawa *et al.*, 1975).

Geology and paragenesis

The paragenesis and fluid inclusion content of specimens 1 (University of Michigan) and 2 (Smithsonian Institution NMNH #R691) were investigated

for the purpose of setting limits on the temperature of formation. Both samples came from the Aar Massif, in particular from the so-called Northern Schists. Hydrothermal veins, in which the pyrrhotites were found, occur in sericite-chlorite schists and in amphibolites (Weibel, personal communication). The pyrrhotite crystals were formed at the end of the Alpine orogenesis in the zone of the greenschist facies (Stalder, personal communication). Specimen 1 came from a tunnel of the hydroelectric plant at Amsteg, Uri in the west-central region of the Aar Massif. In association with the pyrrhotite we found adularia, albite, apatite, calcite, chlorite (chamosite), pyrite, quartz, sphalerite, and sphene. The unique 5C pyrrhotite occurred as small hexagonal prisms between well crystallized adularia, and primarily occupied open cavities. The exact locality of origin of specimen 2 is not known but presumably lies near specimen 1, as the Amsteger tunnel was one of only two localities where fresh pyrrhotite crystals were found (Stalder, personal communication). The mineralogical assemblage is adularia, albite, calcite, hematite, pyrrhotite, and quartz. There are two distinct generations of pyrrhotite. One occurs as sparse, large prisms associated with hematite, while the other consists of numerous, tiny (≤ 0.1 mm) hexagonal plates coating the calcite and adularia. Similarity in grain size, habit, and mineral sequence, as well as essential similarity of fluid inclusions in the quartz and adularia, suggests that both specimens merely represent different examples of the same paragenesis.

Numerous fluid inclusions of both primary and secondary origin occur in the quartz, feldspars, and calcite of this sequence, and limited studies of these were undertaken to evaluate temperatures of deposition of the intergrown pyrrhotites. All inclusions are of a simple two-phase type consisting of liquid H₂O (brine) and a small vapor bubble at room temperature; no liquid CO₂ is visible in any of the inclusions. With methods and equipment described by Kelly and Turneaure (1970), carefully-selected primary inclusions in each mineral were heated and observed to fill (by liquid expansion) at the following temperatures: quartz, 169–177°C; adularia, 149–163°C; calcite, 71–79°C. The filling temperatures decline sys-

Table 1. Composition of the new 5C pyrrhotites in weight percent

Fe	S	Ni	Co	Cu
60.91	38.86	0.14	0.20	0.02
60.24	38.94	0.19	0.16	0.00

tematically through the paragenesis and, although inclusions in the unique 5C pyrrhotite are invisible, it is paragenetically bracketed by the quartz and adularia and thus to a filling temperature range of about 160–170°C. The later, platy pyrrhotite (4C) formed after calcite and presumably therefore below the 71–79°C range.

It should be emphasized that such filling temperatures are not true depositional temperatures, because they are subject to positive corrections for total pressure at the time of mineral growth. Since the original total pressures are unknown, the filling temperatures should be taken only as *minimum* limits for the true growth temperatures. Working with similar materials from Alpine veins in the same general region, Poty *et al.* (1974) obtained similar filling temperatures, but inferred very large total pressures (2.5–3 kbar), which would place the corrected temperatures at about 400°C. Whether their interpretations are correct or not, they underscore the importance of the pressure corrections and the need for caution in assigning depositional temperatures to the pyrrhotites of interest here.

With these limitations in mind, several firm conclusions can still be drawn from the inclusion studies. The work does establish that the new 5C pyrrhotite is definitely hydrothermal in origin and that it formed at temperatures in excess of about 160–170°C. Furthermore, the inclusion data seem to rule out the possibility that it is a naturally-quenched phase, because it was an intermediate precipitate in a systematic cooling sequence. At least, if it was quenched, it must later have been subjected to extensive annealing during deposition of younger adularia and calcite formed at temperatures of at least 149–163°C and 71–79°C, respectively.

Discussion

Bertaut (1953) described the 4C pyrrhotite and found that there are eight vacant and 56 filled iron sites in the unit cell. These vacancies are regularly distributed in every second iron layer. Corlett (1968) inferred that the NA 3C structure came about by stacking of domains with a *c*-axis repeat of 3C parallel to (001). Nakazawa *et al.* (1976) show that the lattice image of NA 3C pyrrhotite is consistent with three domains related by a $(1/3)c$ glide along the *a* axis, although Corlett (personal communication) indicates that the positions of the intense NA 3C superstructure reflections do not correspond to the earlier findings of Nakazawa and Morimoto (1971) and Corlett (1968). High-resolution lattice images of the

5C pyrrhotite show an apparent random distribution of iron vacancies along the *c* axis in comparison with the 4C type (Morimoto *et al.*, 1974). The detailed nature of the ordering of the vacancies in the unique 5C pyrrhotite is not known, but the origin of the non-Bragg superstructure reflections might be similar to that for NA 3C pyrrhotite. However, our new pyrrhotite is not considered to be of the NA type, as it seems to lack a special intensity distribution and twin relation (Morimoto, personal communication).

Nakazawa and Morimoto (1971) and Kissin (1974) have carried out experiments at elevated temperatures using synthetic materials in order to establish the stability relations among the various pyrrhotites. Their results in the region of the composition Fe_9S_{10} are similar. With decreasing Fe content the 5C structure marks the limit of the NC pyrrhotites, and is replaced by coexisting NC+4C pyrrhotites below about 215°C. At approximately 215°C the structure inverts to the NA (NA 3C) structure while composition remains constant. Neither these nor any other authors have described the appearance of a 5C structure with superstructure reflections in non-Bragg positions. The reasons for this are not obvious, but it is possible that the phase relations are subject to change in detail. This system is a difficult one to study at such low temperatures due to slow reaction rates and lack of reversibility. It is also possible that our 5C pyrrhotite formed as a metastable phase. More detailed studies on the equilibrium phase relations and rates of reaction in the region of the pyrrhotite system near Fe_9S_{10} will be necessary to provide a definitive answer to these questions.

A conclusive explanation for the observed diffraction pattern cannot be described. If the pyrrhotite is a single phase, interpretation of the diffraction relations is extremely difficult, as no superstructure is known to give this pattern. It is perhaps also possible that the pyrrhotite is an intergrowth of two different and unknown phases or that it is twinned with A^* parallel to A^* , but we have no direct evidence for such possibilities. However, for our observed diffraction relations no pyrrhotite has been observed which exhibits relationships consistent with such mechanisms. At the present, we cannot determine the precise structural cause for the observed diffraction relations. It is clear, however, that this pyrrhotite exhibits unique features.

Acknowledgments

We are grateful to Dr. Nobuo Morimoto for his helpful and constructive review of the manuscript. The second specimen from

Uri was kindly provided by the Smithsonian Institution National Museum of Natural History. We wish to thank Professor M. Corlett for her comprehensive review and constructive suggestions.

References

- Bertaut, E. F. (1953) Contribution à l'étude des structures lacunaires: la pyrrhotine. *Acta Crystallogr.*, **6**, 557-561.
- Burnham, C. W. (1965) Refinement of lattice parameters using systematic correction terms. *Carnegie Inst. Wash. Year Book*, **64**, 200-202.
- Carpenter, R. H. and G. A. Desborough (1964) Range in solid solution and structure of naturally occurring troilite and pyrrhotite. *Am. Mineral.*, **49**, 1350-1365.
- Corlett, M. (1968) Low iron polymorphs in the pyrrhotite group. *Z. Kristallogr.*, **126**, 124-134.
- Kelly, W. C. and F. S. Turneaure (1970) Mineralogy, paragenesis and geothermometry of the tin and tungsten deposits of the eastern Andes, Bolivia. *Econ. Geol.*, **65**, 609-680.
- Kissin, S. A. (1974) *Phase Relations in a Portion of the Fe-S System*. Ph.D. Dissertation, University of Toronto, Canada.
- Morimoto, N., H. Nakazawa, M. Tokonami and K. Nishiguchi (1971) Pyrrhotites: structure type and composition. *Soc. Mining Geol. Japan, Special Issue 2*, 15-21.
- , —— and E. Watanabe (1974) Direct observation of metal vacancy in pyrrhotite, $Fe_{1-x}S$, by means of an electron microscope. *Proc. Japan Acad.*, **50**, 756-759.
- , G. Atsuo, T. Koji and K. Koto (1975a) Superstructure and non-stoichiometry of intermediate pyrrhotites. *Am. Mineral.*, **60**, 240-248.
- , A. Gyobu, H. Mukaiyama and E. Izawa (1975b) Crystallography and stability of pyrrhotites. *Econ. Geol.*, **70**, 824-833.
- Nakazawa, H. and N. Morimoto (1971) Phase relations and superstructures of pyrrhotite, $Fe_{1-x}S$. *Mater. Res. Bull.*, **6**, 345-358.
- , ——, and E. Watanabe (1975) Direct observation of metal vacancies by high resolution electron microscopy. Part I: 4C type pyrrhotite (Fe_7S_8). *Am. Mineral.*, **60**, 359-366.
- , —— and —— (1976) Direct observation of iron vacancies in polytypes of pyrrhotite. In H. R. Wenk, Ed., *Electron Microscopy in Mineralogy*, p. 304-309. Springer-Verlag, Berlin.
- Poty, B. P., H. A. Stalder and A. M. Weisbrod (1974) Fluid inclusion studies in quartz from fissures of western and central Alps. *Schweiz. Mineral. Petrogr. Mitt.*, **54**, 717-752.
- Rucklidge, J. C. and E. L. Gasparrini (1969) *EMPADR VII Specifications of the Computer Programme for Processing Electron Microprobe Analytical Data*. Department of Geology, University of Toronto, Canada.
- Tokonami, M., K. Nishiguchi and N. Morimoto (1972) Crystal structure of a monoclinic pyrrhotite (Fe_7S_8). *Am. Mineral.*, **57**, 1066-1080.

Manuscript received, September 26, 1977; accepted for publication, April 13, 1978.